Blocking Analysis in Hybrid TDM-WDM Passive Optical Networks

John S. Vardakas, Vassilios G. Vassilakis and Michael D. Logothetis

***Abstract*—Optical access networks are the ultimate solution to the problem of the last mile bottleneck between high-capacity metro networks and customer premises, capable of delivering future integrated broadband services. Nowadays, passive optical networks are the most promising and cost-effective class of fiber access systems. This rapid evolvement of fiber in access networks motivates the study of their performance. In this paper we develop teletraffic loss models for calculating connection failure probabilities (due to unavailability of a wavelength) and call blocking probabilities (due to the restricted bandwidth capacity of a wavelength) in hybrid TDM-WDM passive optical networks with dynamic wavelength allocation. The springboard of our analysis is well-established recursive teletraffic models. The proposed models are derived from one-dimensional Markov chains which describe the wavelengths occupancy in the optical access network. The optical access network accommodates multiple service-classes with infinite or finite number of traffic sources. The accuracy of the proposed models is validated by simulation and was found to be absolutely satisfactory.**

***Index Terms*— Wavelength division multiplexing, passive optical networks, blocking probability, Markov chains, Poisson, quasi-random.**

I. Introduction

THE increased demand for more bandwidth and the expansion of the telecommunication services offered to residential homes, have forced conventional access network infrastructures, like Digital Subscriber Line (DSL) systems, to the edge of their capabilities [1]. The final option for access technology is optical fiber, due to its unique properties, providing huge bandwidth with very low loss.

Optical access networks can be classified into three general categories [2]. In the Point-to-Point (PtP) architecture, a dedicated fiber is used to connect directly the customers to the central office. This approach is effective in terms of bandwidth, but it has the limitation of high cost of the network user's equipment, which must realize Optical-Electrical-Optical (OEO) conversions. A second access solution is the active star architecture, a shared fiber approach, where a fiber is used to connect the central office with an active node, placed at the location of the network users. In a third solution, the active node is replaced with a passive splitter/combiner in passive star architectures, reducing the cost of the power supply and maintenance in the active node. Passive Optical Networks (PONs) have gained prominence and are reported as the optimum solution for utilizing the advantages of optical fibers in access networks [3]. PONs are already deployed today, including their application to the Fiber-To-The-Home / Fiber-To-The Premises (FTTH / FTTP) networks [4].

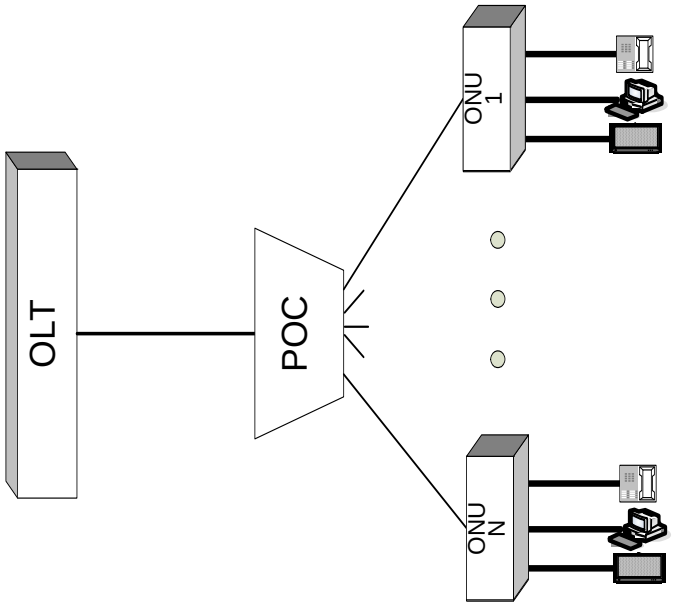

Fig. 1: A basic PON architecture.

A PON consists of an Optical Line Terminal (OLT), located at the central office and optical nodes which are located in the customers' premises and called Optical Network Units (ONUs) [5]. All ONUs are connected to the OLT through a combiner/splitter which we call Passive Optical Concentrator (POC); the communication between the ONUs is realized only through the OLT (Fig. 1). The POC is a passive device, where signals from the ONUs are combined and transmitted to the OLT with one fiber; signals from the OLT are separated and then sent to ONUs. In other words, in the downstream direction (from the OLT to the ONUs) traffic is sent from one point to multiple points, while in the upstream direction (from the ONUs to the OLT), traffic from multiple points, reaches only one point. In both directions, different multiplexing

This work was supported by the project ΠΕΝΕΔ-No.03ΕΔ420, which is funded in 75% by the European Union – European Social Fund and in 25% by the Greek State – General Secretariat for Research and Technology.

All authors are with the WCL, Dept. of Electrical and Computer Engineering, University of Patras, 265 04 Patras, Greece
(corresponding author: M. D. Logothetis, +302610996433; fax: +302610991855; e-mail: m-logo@wcl.ee.upatras.gr).

techniques are introduced, in order to provide high utilization of the fiber bandwidth capacity. In Time Division Multiplexing (TDM) PONs, the optical signals from the ONUs are transmitted in different time slots, in order to avoid collisions and are multiplexed at the passive element. Time-based architectures that have been already deployed are Asynchronous Transfer Mode PONs (ATM-PONs), Ethernet PONS (EPONs) and Broadband PONs (BPONs). These architectures use a 1550 nm wavelength for the downstream traffic and a 1310 nm for the upstream traffic [6]. Given the steadily increasing number of users and their bandwidth demands, current TDM-PONs must be upgraded in order to satisfy these growing traffic demands. One approach refers to the increase of the line rate of the existing TDM architectures. The Gigabit-capable PON (GPON) is specified by the International Telecommunications Union-Telecommunication Standardization Sector (ITU-T) G.984 [7]. GPON is capable of providing higher bandwidth, namely a line rate of 2.4 Gbps downstream and 1.2 Gbps upstream, supporting up to 64 users. Another upgrading approach for the TDM-PONs is to combine the Wavelength Division Multiplexing (WDM) technology together with the TDM technology. In the resulting hybrid TDM-WDM PON, multiple wavelengths are used in the upstream and downstream directions, so that the access network becomes flexible and efficient in providing the required bandwidth to the users [8]. In early TDM-WDM PONs systems, each ONU uses expensive optical transmitters, generating a unique wavelength. Cost-effective approaches [1], [9] make TDM-WDM PONs the ideal solution for broadband access networks.

In this paper, we develop analytical loss models for calculating blocking probabilities in the upstream direction of a hybrid TDM-WDM PON, with dynamic wavelength allocation. In order for an ONU to be connected with the OLT, a free wavelength must be seized in the PON (actually the problem of finding a free wavelength is localized in the link between the POC and the OLT). We calculate the Connection Failure Probability (CFP), which occurs due to the unavailability of a free wavelength in the link between the POC and the OLT. We also calculate the Call Blocking Probability (CBP) that occurs after the establishment of the OLT-ONU connection, due to the restricted bandwidth capacity of a wavelength. We consider that calls belong to different service-classes with infinite or finite traffic source population. The number of ONUs is finite, but large enough, so that they are more than the number of wavelengths in the PON. This consideration is done in order for our study to be meaningful (despite of the fact that it is also realistic). The proposed models are computationally efficient, because they are based on recursive formulas. Our analysis is validated through simulation; the accuracy of the proposed models was found to be quite satisfactory.

This paper is organized as follows. In section 0 we describe the basic features of our service model, while in sections III and IV we present the analytical models for the infinite and finite traffic-sources cases, respectively. Section V is the evaluation section. We conclude in section VI.

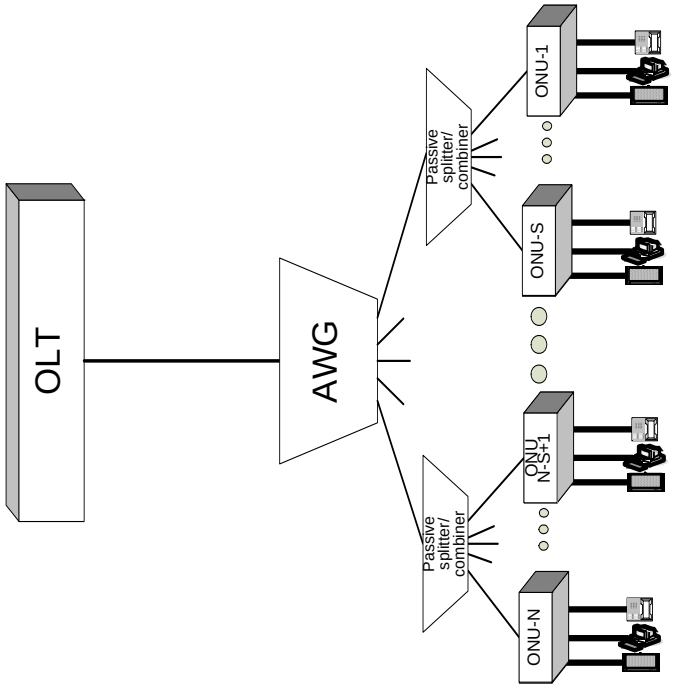

Fig. 2: Architecture of a hybrid TDM-WDM PON with multistage splitting technique.

II. Service Model Of The Hybrid TDM-WDM PON

We consider a hybrid TDM-WDM PON with multistage splitting, as shown in Fig. 2. Multistage splitting is a technique that is used for increasing the utilization of the wavelength's bandwidth capacity. Thanks to dynamic wavelength allocation scheme that is applied to the PON, each ONU has the ability of connecting to the OLT by using any available wavelength; in contrast to the static wavelength allocation scheme where a certain wavelength is assigned to an ONU. The POC comprises a Passive Wavelength Router (PWR) which is responsible for routing multiple wavelengths in a single fiber toward the OLT.

The connection establishment procedure of an ONU to the OLT is as follows. When a call arrives to an ONU while no other calls either of the same ONU or the other ONUs in the group are in service, it searches for an available wavelength in the PON. This is actually done through connection setup signals between the OLT and the ONU; a free wavelength is found by the OLT and is assigned to the group of ONUs and to the call. Then, a connection is established and the call is serviced, otherwise (if the search of a free wavelength is unsuccessful) the call is blocked and lost (connection failure occurs). Since after the connection establishment, all calls from the same ONU group seize the same wavelength, while the bandwidth capacity of the wavelength is restricted, call blocking occurs. When all calls on a wavelength terminate, the connection also terminates and the wavelength releases its resources to become available to any new arriving call from any ONU group.

In the following sections we present analytical models for the CFP and the CBP in the upstream transmission, namely

the direction from the ONUs to the OLT, while assuming that each ONU accommodates multiple service-classes with infinite or finite number of traffic sources. The presented models involve the number of the ONUs per splitting device in a parametric way, therefore, they can also be applied to the case where the hybrid TDM-WDM PON is implemented with one-stage splitting as shown in Fig. 1.

III. Models for Service-Classes with Infinite Number of Traffic Sources

Let C be the number of different wavelengths and N be the number of ONUs in the PON of Fig. 2. Each splitting device supports a group of S ONUs ($S<N$); therefore the number of the splitters in the access network is N/S (where N is a multiple of S). Each wavelength has a bandwidth capacity of T bandwidth units (b.u.). Calls arrive to the ONU according to a Poisson process and are groomed onto one wavelength. Each ONU accommodates K service-classes. In order for each service-class call to be serviced, it requires b_k $(k=1,...,K)$ b.u. of the wavelength. The b.u. of each wavelength are commonly shared among the arriving calls. If the requested b.u. of a call are not available, the call is blocked and lost (Complete Sharing policy [10]). The arrival rate of service-class k call is denoted by λ_k, while the service time is exponentially distributed with mean μ_k^{-1}.

In order to derive the CFP, we formulate a Markov chain with the state transition diagram of Fig. 3, where the stage j represents the number of occupied wavelengths in the PON. We denote the total arrival rate of calls from an ONU by $\lambda=\sum_{k=1}^{K}\lambda_k$. The establishment of a connection is realized with a rate that depends on the number of the ONUs, which have not established a connection yet. Having established a connection of one ONU, we have actually connected all ONUs of the same group. Therefore, after one connection establishment, the number of ONUs, which have not established a connection, is reduced by S (the number of ONUs in a group). Because of this, when the system is in state [j-1], it will jump to the state [j] (N-(j-1)S)λ times per unit time (Fig. 3), where N-(j-1)S is the number of ONUs which have not been connected yet.

In order to define the rate by which a wavelength is released, we must consider not only the number of the occupied wavelengths j, but also the fact that the release of a wavelength coincides with the release of the last call, which seizes the wavelength and may belong to any service-class. The downward transition from state [j] to state [j-1] is realised jQ times per unit time, where Q corresponds to the mean service/seize rate of a wavelength. The rate Q can be determined by the product of (the conditional probability that b_k b.u. are occupied in the wavelength by only one call of service-class k, given that the wavelength is occupied) by (the corresponding service rate μ_k). Since the last call could belong to any service-class:

$$Q=\sum_{k=1}^{K}\mu_k y_k(b_k)\frac{q(b_k)}{\sum_{i=1}^{T}q(i)} \tag{1}$$

where:

$y_k(b_k)$ is the mean number of service-class k calls (with bandwidth requirement b_k) when b_k b.u. are occupied in the wavelength, and

$q(i)$ is the occupancy distribution of the b.u. in a wavelength, which can be calculated by the well-known Kaufman-Roberts recursion for service-classes with infinite traffic-source population [11], [12]:

$$iq(i)=\sum_{k=1}^{K}a_k b_k q(i-b_k), \text{ for } i=1,...,T \tag{2}$$

with $q(i)=0$ for $i<0$ and $\sum_{i=0}^{T}q(i)=1$. The offered traffic-load a_k for service-class k comes from the group of S ONUs, therefore:

$$a_k=S\lambda_k\mu_k^{-1} \tag{3}$$

where the product $\lambda_k\mu_k^{-1}$ represents the offered traffic-load of one ONU. This is possible due to the Poisson process.

The mean number of service-class k calls is given by [12]:

$$y_k(i)=\frac{a_k q(i-b_k)}{q(i)} \tag{4}$$

The probability $P(j)$ that j wavelengths are occupied in the link can be derived from the rate balance equations of the state transition diagram of Fig. 3. A method for deriving the distribution $P(j)$ can be found in [10]. More specifically, from the rate-out = rate-in, we get the steady state equation:

$$\begin{aligned}(N-(j-1)S)\lambda P(j-1)+[(j+1)Q]P(j+1)=\\ [(N-jS)\lambda+jQ]P(j)\end{aligned} \tag{5}$$

where $P(j)=0$ for $j<0$ and $j>C$. By summing up side by side of (5) from $j=0$ to $j-1$, we get the recurrence formula:

$$P(j)=\frac{\lambda}{Q}\frac{N-(j-1)S}{j}P(j-1) \tag{6}$$

Consecutive applications of (6) yields to the equation:

$$P(j)=\left(\frac{\lambda}{Q}\right)^{j}\cdot\frac{\prod_{i=1}^{j}[N-(j-1)S]}{j!}\cdot P(0) \tag{7}$$

where $P(0)$ is the probability that no wavelengths are in service. Using the normalization condition,

$$\sum_{j=0}^{C} P(j)=1 \tag{8}$$

it follows that:

$$P(0)=\left[\sum_{l=0}^{C}\left(\frac{\lambda}{Q}\right)^{l}\frac{\prod_{j=1}^{l}[N-(j-1)S]}{l!}\right]^{-1} \tag{9}$$

Therefore, by using (7) and (9), we get the wavelength occupancy distribution in the PON:

$$P(j)=\left(\frac{\lambda}{Q}\right)^{j}\cdot\frac{\prod_{i=1}^{j}[N-(j-1)S]}{j!}\cdot\left[\sum_{l=0}^{C}\left(\frac{\lambda}{Q}\right)^{l}\frac{\prod_{j=1}^{l}[N-(j-1)S]}{l!}\right]^{-1} \tag{10}$$

The CFP is determined by $P(C)$, since a connection establishment is blocked and lost if and only if all the wavelengths are occupied.

To calculate the CBP B_k of service-class k calls of a particular ONU utilizing the access network, we rely on (2) while summing up the last b_k $q(i)$'s which correspond to the blocking states:

$$B_k=\sum_{j=T-b_k+1}^{T} q(j) \tag{11}$$

Note that the above model can be easily applied to the one-stage splitting case by setting $S=1$.

IV. Models for Service-Classes with Finite Number of Traffic Sources

In the aforementioned service model of the Hybrid TDM-WDM PON, we now consider that each service-class has a finite source population; let M_k be the number of traffic sources of service-class k. To analyze the new model, we use the Markov chain of the corresponding infinite model (Fig. 3), while properly modifying the parameters λ and Q.

In what follows, we show that the state transition diagram of Fig. 3 can also represent the Markov chain for the new service model with service-classes of finite population. Due to the finite traffic source population the call arrival process in each ONU is not random (Poisson) but we consider it quasi-random. The arrival rate of an idle traffic source of service-class k is denoted by v_k. If no call is in service in each ONU, then the effective arrival rate to each ONU from service-class k is $M_k v_k$, and the total call arrival rate to each ONU becomes $\lambda=\sum_{k=1}^{K} M_k v_k$.

The establishment of a connection can be realized by any call (from any service-class) that arrives from an ONU (belonging to an ONU group). Hence, the transition from state [j-1] to state [j], takes place $\left(N-(j-1)S\right)\lambda$ times per unit time; where N-(j-1)S is the number of ONUs which have not been connected yet. The reverse transition, from state [j] to state [j-1], is realized jQ times per unit time, where the service rate of the wavelength Q is given as in (1), by:

$$Q=\sum_{k=1}^{K}\mu_k y_{k_F}(b_k)\frac{q_F(b_k)}{\sum_{i=1}^{T} q_F(i)} \tag{12}$$

where:

$y_{k_F}(b_k)$ is the mean number of service-class k calls (with bandwidth requirement b_k) when b_k b.u. are occupied in the wavelength;

$q_F(i)$ is the occupancy distribution of the b.u. in a wavelength, for finite number of traffic sources per service-class.

The mean number of service-class k calls, $y_{k_F}(i)$, when i b.u. are occupied in the wavelength is given by:

$$y_{k_F}(i)=\frac{a_{k_F} q_F(i-b_k)}{q_F(i)} \tag{13}$$

where $a_{k_F}=v_k\mu_k^{-1}$ is the offered traffic-load per idle source of service-class k.

Since S ONUs utilize the same wavelength, the overall number of sources of the service-class k that demand service within one wavelength is $S\cdot M_k$. Therefore, the occupancy distribution of i b.u., $q_F(i)$, is given by the following recurrent formula, according to the Engset Multi-rate Loss model (EnMLM) [13], [14]:

$$iq_F(i)=\sum_{k=1}^{K} a_{k_F} q_F(i-b_k)\left(S\cdot M_k-n_k(i)+1\right) \text{ for } i=1,...T, \tag{14}$$

$q_F(i)=0$ for $\imath<0$ and $\sum_{i=0}^{T} q_F(i)=1$.

In (9) $n_k(i)$ is the number of service-class k calls which are in service when i out of T b.u. are seized in the wavelength. It has been proved ([15]) that this number can be approximated by $y_k(i)$, the average number of service-class k calls in the corresponding system, when infinite population is assumed for each service-class. In the corresponding system with infinite traffic sources, the offered traffic-load of service-class k is $S\cdot M_k a_{k_F}$; therefore, as in (4), we get:

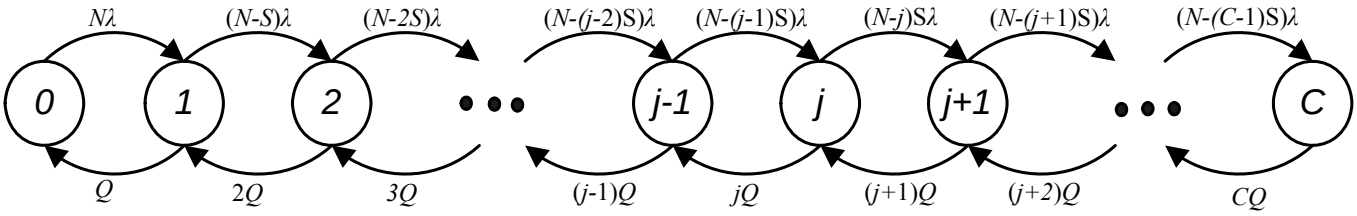

Fig 3: State transition diagram of a TDM-WDM PON with C wavelengths and dynamic wavelength assignment.

$$n_k(i) \approx y_k(i) = \frac{SM_k a_{k_F} q(i-b_k)}{q(i)} \qquad (15)$$

where $q(i)$ is the occupancy distribution of the b.u. of a wavelength, for the infinite traffic-sources case, and is given by (2). Note that the offered traffic-load in (2) is substituted with $S \cdot M_k a_{k_F}$.

The probability $P(j)$ that j wavelengths are occupied in the PON in steady state can be derived from the rate balance equations of the state transition diagram of Fig. 3. Thereupon, the CFP is obtained by (10), as $P(C)$, when $\lambda = \sum_{k=1}^{K} M_k v_k$ and Q is determined by (12). For an ONU utilizing the PON, the CBP B_{k_F} of service-class k calls is calculated, as Time Congestion Probability ([10]), by:

$$B_{k_F} = \sum_{j=T-b_k+1}^{T} q_F(j) \qquad (16)$$

V. Evaluation

In this section we evaluate the proposed models through simulation. To this end, we consider a hybrid TDM-WDM PON with $N = 100$ ONUs and capacity $C = 32$ wavelengths. The bit rate of the upstream direction is selected to be 155 Mbps, therefore, assuming that $1\,\text{b.u.} = 1\,\text{Mbps}$, the wavelength capacity is $T = 155\,\text{b.u.}$ The ONUs form groups with $S = 2$, that is, one wavelength is shared by 2 ONUs. The PON accommodates three service-classes, s_1, s_2 and s_3, with bandwidth requirements $b_1 = 48$ b.u, $b_2 = 36$ b.u and $b_3 = 24$ b.u., respectively. The simulation results are obtained as mean values from 8 runs with confidence interval of 95%.

We consider two cases of service-classes, the first case with infinite and the second case with finite population. In the first case of infinite population, we comparatively present analytical and simulation results for the CFP and CBP, versus the offered traffic-load, in Table 1. The analytical CFP results are obtained through (1), (2), (3), (4) and (9), whereas the analytical CBP results are obtained through (2), (3) and (11). The results of Table 1 show a completely satisfactory accuracy of the proposed model.

In the second case of finite population, the same number of traffic-sources is assumed for all service-classes: $S_1 = S_2 = S_3 = 10$. In Table 2, we comparatively present analytical and simulation results for the CFP and CBP, versus the offered traffic-load. The analytical CFP results are obtained through (2), (10), (12), (13), (14) and (15), whereas the analytical CBP results are obtained through (14) and (16). As the results of Table 2 reveal, the accuracy of the proposed models is completely satisfactory. The small divergence between the analytical and simulation results is an outcome of the approximation that is introduced in the models for the calculation of $n_k(i)$. Nevertheless, this discrepancy is minor and in a well-acceptable level.

The results of Table 2 can be compared to the results of Table 1, because we have considered an equal offered traffic-load each time; i.e. $a_1 = S_1 a_{1_F}$, $a_2 = S_2 a_{2_F}$ and $a_3 = S_3 a_{3_F}$. Comparing the results of Table 1 to the results of Table 2, one can observe that the CFP of the finite population case are higher than the corresponding results of the infinite population case. The reverse situation happens for the CBP results; higher CBP are obtained for infinite population. Both CFP and CBP results are reasonable. When lower CBP results are obtained for finite traffic sources, it means that more calls are serviced by a wavelength and therefore the mean service/seize time of the wavelength is increased, or, in other words, the CFP is increased. The consistence of the results validates our models.

Having validated the models and evaluated their accuracy through simulation, we proceed to investigate the effect of the number of ONUs, N, and the wavelength capacity T to the CFP. Fig. 4 and 5 correspond to infinite and finite traffic-sources cases, respectively, and show the variation of the CFP versus the number of ONUs, N, for three wavelength capacities: $T = 80$, 100 and 155 b.u. In the infinite traffic sources case, the offered traffic-load for s_1, s_2 and s_3, is $a_1 = 0.08$ erl, $a_2 = 0.12$ erl and $a_3 = 0.18$ erl, respectively. In the case of finite population, the number of traffic sources of s_1, s_2 and s_3, is $S_1 = S_2 = S_3 = 5$, while the offered traffic-load per idle source is $a_{1_F} = 0.016$ erl, $a_{2_F} = 0.024$ erl and $a_{3_F} = 0.032$ erl, respectively. As it was anticipated (Fig. 4 and 5) the increase of the number of ONUs strongly increases the CFP, especially when the wavelength bandwidth capacity T is large. This is due to the fact that the increase of the ONUs leads to higher demand

for connections in the PON and therefore to higher CFP. The decrease of *T* leads to smaller CFP, since the release of a wavelength is more frequent when the values of *T* are small, given that the other traffic parameters are the same.

VI. Conclusion

In summary, we propose teletraffic loss models, for hybrid TDM-WDM PONs with dynamic wavelength allocation that accommodate service-classes of infinite or finite number of traffic-sources. The proposed models are derived from one-dimensional Markov chains, which describe the wavelengths occupancy in the PON. The analytical calculations of CFP and CBP are based on the systems state distributions. The models are validated and evaluated through extensive simulation, based on the results. Their accuracy was found to be absolutely satisfactory. Based on the proposed models, several investigations could be carried out, as for example, we showed the impact of the number of ONUs and the wavelength bandwidth capacity on the CFP. In our future work we shall extend our research by considering queues in each ONU while including in our study not only the upstream but also the downstream direction (from OLT to the ONUs).

Acknowledgement

The authors would like to thank Dr Ioannis D. Moscholios (University of Patras, Greece) for his support.

References

[1] F. Effenberger, D. Cleary, O. Haran, G. Kramer, R. Ding Li, M. Oron, T. Pfeiffer, "An Introduction to PON Technologies", *IEEE Communications Magazine,* pp. S17-S25, March 2007.

[2] B. Mukherjee, "*Optical WDM Networks*", Springer, 2006.

[3] T. Koonen, "Fiber to the Home/Fiber to the Premises: What, Where, and When?", *Proceedings of the IEEE*, Vol. 94, No. 5, pp. 911-934, May 2006.

[4] M. Abrams, P. C. Becker, Y. Fujimoto, V. O'Byrne, and D. Piehler, "FTTP Deployments in the United States and Japan-Equipment Choices and Service Provider Imperatives", *IEEE/OSA Journal of Lightwave Technology*, Vol. 23, No. 1, pp. 236-246, January 2005.

[5] R. Davey, F. Bourgart, K. McCammon, "Options for Future Optical Access Networks", *IEEE Communications Magazine*, October 2006.

[6] M. Ma, Y. Zhu, and T. H. Cheng, "A Systematic Scheme for Multiple Access in Ethernet Passive Optical Networks", *IEEE/OSA Journal of Lightwave Technology*, Vol. 23, No. 11, pp. 3671-3682, November 2005.

[7] ITU-T G.984.1, SG 15, "Gigabit-Capable Passive Optical Networks (G-PON): General Characteristics," March 2003.

[8] A. R. Dhaini, C. M. Assi, M. Maier and A. Shami, "Dynamic Wavelength and Bandwidth Allocation in Hybrid TDM/WDM EPON Networks", *IEEE/OSA Journal of Lightwave Technology*, Vol. 25, No. 1, pp.277-286, January 2007.

[9] D. Gutierrez, W.-T. Shaw, F.-T. An, K. S. Kim, Y.-L. Hsueh, M. Rogge, G. Wong and L. G. Kazovsky, "Next generation optical access networks", (Invited Paper), *Proceedings of IEEE/Create-Net BroadNets 2006*, Oct. 2006.

[10] H. Akimaru, K. Kawashima, *Teletraffic – Theory and Applications*, Springer-Verlag, 1993.

[11] J. S. Kaufman, "Blocking in a shared resource environment", *IEEE Transactions on Communications,* Vol.29, No. 10, pp.1474-1481, October 1981.

[12] I. Moscholios, M. Logothetis, G. Kokkinakis, "Connection Dependent Threshold Model: A Generalization of the Erlang Multiple Rate Loss Model," *Performance Evaluation, Special issue on "Performance Modeling and Analysis of ATM & IP Networks"*, Vol. 48, issue 1-4, pp. 177-200, May 2002.

[13] G. Stamatelos and J. Hayes, "Admission control techniques with application to broadband networks", *Computer Communications,* (17), (9), pp. 663-673, 1994.

[14] I .D. Moscholios, M. D. Logothetis, and P. I. Nikolaropoulos, "Engset multi-rate state-dependent loss models", *Performance Evaluation,* Vol.59, Issues 2-3, pp. 243-277, February 2005.

[15] M. Glabowski and M. Stasiak, "An Approximate Model of the Full-Availability Group with Multi-Rate Traffic and a Finite Source Population", *Proc. of 12th MMB&PGTS*, Germany, 12-15 Sept. 2004.

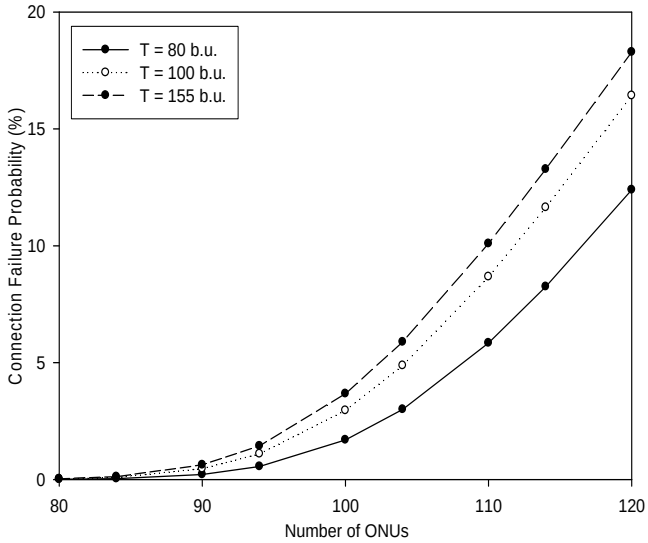

Fig. 4: CFP versus the number of ONUs for different values of the wavelength bandwidth capacity *T*, for the infinite number of traffic sources case.

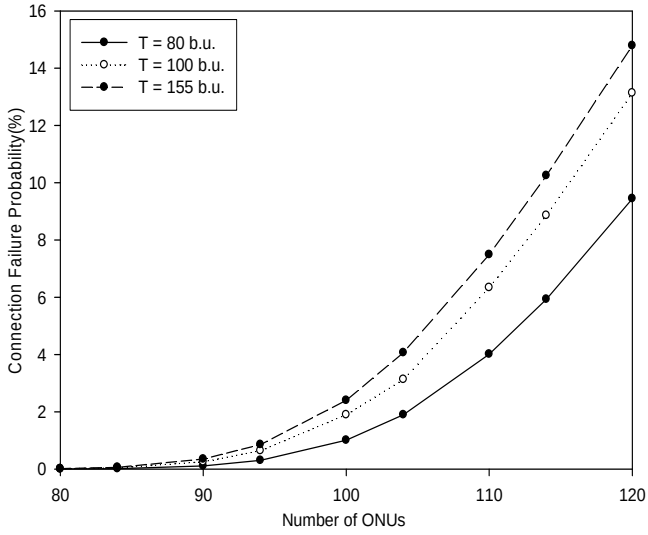

Fig. 5: CFP versus the number of ONUs for different values of the wavelength bandwidth capacity *T*, for the finite number of traffic sources case.

TABLE I
ANALYSIS VERSUS SIMULATION FOR THE INFINITE TRAFFIC-SOURCES CASE

Traffic-Load (erl)			CFP			CBP 1st service-class			CBP 2nd service-class			CBP 3rd service-class		
				Simulation			Simulation			Simulation			Simulation	
a_1	a_2	a_3	Analysis (%)	Mean (%)	95% Conf. Interval	Analysis (%)	Mean (%)	95% Conf. Interval	Analysis (%)	Mean (%)	95% Conf. Interval	Analysis (%)	Mean (%)	95% Conf. Interval
0.04	0.060	0.090	0.00019	0.00125	0.000053	0.296648	0.23544	0.012999	0.150786	0.122189	0.007612	0.058591	0.05074	0.00563
0.05	0.075	0.1125	0.010532	0.02303	0.00401	0.548903	0.53826	0.025791	0.286242	0.285086	0.011151	0.11645	0.11810	0.00634
0.06	0.09	0.135	0.161948	0.17918	0.005699	0.897703	0.89889	0.013748	0.479255	0.477203	0.006664	0.202868	0.20379	0.00400
0.07	0.105	0.1575	1.043973	1.07559	0.019481	1.347999	1.35111	0.029188	0.735378	0.732316	0.014098	0.32229	0.32242	0.00611
0.08	0.120	0.180	3.672296	3.72838	0.040493	1.901324	1.90925	0.034634	1.058163	1.048074	0.02411	0.47822	0.47822	0.00706
0.09	0.135	0.2025	8.540600	8.62377	0.075234	2.556398	2.54561	0.037499	1.449397	1.438622	0.016823	0.673198	0.67334	0.01644
0.10	0.150	0.225	15.13064	15.1707	0.060469	3.309697	3.31048	0.053834	1.90903	1.906029	0.035339	0.908823	0.91952	0.01473

TABLE II
ANALYSIS VERSUS SIMULATION FOR THE FINITE TRAFFIC-SOURCES CASE

Traffic-Load (erl) per idle source			CFP			CBP 1st service-class			CBP 2nd service-class			CBP 3rd service-class		
				Simulation			Simulation			Simulation			Simulation	
a_{1_F}	a_{2_F}	a_{3_F}	Analysis (%)	Mean (%)	95% Conf. Interval	Analysis (%)	Mean (%)	95% Conf. Interval	Analysis (%)	Mean (%)	95% Conf. Interval	Analysis (%)	Mean (%)	95% Conf. Interval
0.004	0.006	0.009	0.000197	0.00118	0.000263	0.297799	0.26982	0.011795	0.150821	0.130392	0.00598	0.058028	0.04886	0.004466
0.005	0.0075	0.01125	0.010909	0.08952	0.005689	0.551499	0.49694	0.014714	0.286845	0.253134	0.01102	0.115735	0.102	0.004717
0.006	0.009	0.0135	0.167063	0.15812	0.018605	0.902304	0.81299	0.025324	0.480777	0.418628	0.01515	0.202034	0.17490	0.010594
0.007	0.0105	0.01575	1.071191	1.03050	0.045236	1.354981	1.24621	0.031856	0.738068	0.642812	0.02313	0.321311	0.28054	0.009839
0.008	0.012	0.018	3.746995	3.54465	0.113104	1.910786	1.71606	0.029119	1.062092	0.917005	0.01657	0.476971	0.40643	0.012139
0.009	0.0135	0.02025	8.671605	8.29533	0.139682	2.568112	2.39401	0.040406	1.45435	1.322734	0.02236	0.631424	0.58117	0.009107
0.01	0.015	0.0225	15.30373	14.6961	0.117506	3.233093	2.97334	0.037112	1.914714	1.704498	0.06205	0.906125	0.81465	0.045787